Revista Eletrônica Paulista de Matemática

ISSN 2316-9664
v. 22, n. 2, set. 2022
Edição Brazilian Symposium on Fractional Calculus

Micaeli Mendola Theodoro
IBB - Instituto de Biociências
UNESP - Universidade Estadual Paulista "Júlio de Mesquita Filho"
micaeli.theodoro@unesp.br

Thomas Nogueira Vilches
Agent-Based Modelling Laboratory
York University, Toronto, Ontario, Canada
thomvilches@gmail.com

Rubens de Figueiredo Camargo
Faculdade de Ciências
UNESP - Universidade Estadual Paulista "Júlio de Mesquita Filho"
rubens.camargo@unesp.br

Paulo Fernando de Arruda Mancera
IBB - Instituto de Biociências
UNESP - Universidade Estadual Paulista "Júlio de Mesquita Filho"
paulo.mancera@unesp.br

Fractional modeling of COVID-19 dynamics

Abstract

The present work seeks to provide a comparison between the classical epidemiological model using ordinary differential equations and an approach through the fractional calculus, using the COVID-19 pandemic in Brazil as a case study. To do that,we propose a classic SAIRD (susceptible-asymptomatic-symptomatic-recovered-dead) model and its fractional generalization, and we used the B_1 method and the mean squared error to compare and demonstrate which model and strategy is more accurate reproducing the data of COVID-19 in Brazil.

Keywords: Fractional Modeling. Population Dynamics. Computational Strategies. Numerical Methods. COVID-19.

1 Introduction

At the end of December 2019, an outbreak of pneumonia characterized by fever, dry cough, fatigue, and occasional gastrointestinal problems started at the Huanan seafood wholesale market in Wuhan, Hubei, China, involving around 66% of the employees. On the first day of 2020, the market was closed and, even with the closure, thousands of people in different Chinese provinces, such as Hubei, Zhejiang, Guangdong, Henan, were infected. Cities like Beijing and Shanghai were also affected and later the infections, caused by a virus, reached other countries like Thailand, South Korea, Vietnam, Germany, the United States and Singapore (WU; CHAN, 2020). The virus was identified as a new coronavirus that causes a Severe Acute Respiratory Syndrome (SARS) and was named as SARS-CoV-2, in reference to the SARS-CoV, which spread between 2002 and 2003 around the world (WU; CHAN, 2020; CHAKRABORTY; MAITY, 2020).

On March 11, 2020, the so called COVID-19 (*Coronavirus Disease 2019*), caused by SARS-CoV-2, was considered a pandemic by World Health Organization (WHO). According to data from the WHO, on November 28, 2021, the world accounts for 261,075,046 cases and 5,195,138 deaths due to the disease around the world.

The COVID-19 pandemic destabilized the whole world in the most diverse instances, generating a crisis in public health, politics, economy, and mental health. Just like in the world, the situation in Brazil has been extremely serious. The first case of COVID-19 was detected on February 26, 2020 and, since there, we counted 22,076,863 cases and 614,186 deaths due to COVID-19, according to the Ministry of Health (BRASIL, 2021)

The transmission of SARS-CoV-2 occurs through airways, droplets and aerosols, usually due to the proximity between susceptible persons and infectious ones. Even those infected individuals with no obvious symptoms can transmit the virus, and it is estimated that about 80% of those infected with SARS-CoV-2 are asymptomatic (SANTOS, 2020). Some measures can reduce the spread such as frequent hand washing, social distancing, use of masks covering the mouth and nose, in addition to cleaning surfaces (SANTOS, 2020).

Within the context of infectious diseases, mathematical modeling plays a major role in understanding the cellular dynamics or the spread of a disease in the population. More specifically, in the case of COVID-19, several mathematicians, epidemiologists and researchers from all over the world have engaged in using real data, performing curve adjustments, as well as making predictions about the progress of the pandemic in the most diverse locations. In the present work we seek to analyze the spread dynamics of COVID-19 using a SAIRD model and its fractional generalization.

The general objective of this work is the study of mathematical modeling through differential equations and different techniques to improve it. More precisely, the study of the so-called fractional modeling, that is, the modeling made by differential equations of non-integer order, aiming its use to describe the population dynamics of COVID-19 in Brazil, using Caputo's derivative of non-integer order, to performing curve adjustments based on real data available (COTA, 2020), in accordance with official sources.

2 Classic mathematical modeling for COVID-19

According to (KISS; MILLER; SIMON, 2017), infectious diseases may cause serious health and economic crises, and mathematical modeling allows us to guide public and individual policy responses to control these diseases. Since the beginning of the COVID-19 pandemic, many mathematical models have been presented to help the authorities to design mitigation strategies. Here, we present a susceptible-asymptomatic-symptomatic-recovered model that account for the deaths due to the COVID-19 infection. The model is schematized in Figure 1.

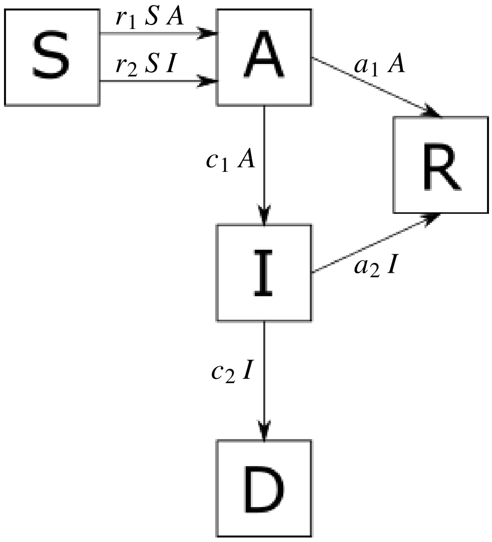

Figure 1: Schematic of compartments of the SAIRD model.

With the associated Ordinary Differential Equation system given by:

$$\begin{cases} \frac{dS}{dt} = -r_1\,S\,A - r_2\,S\,I \\ \frac{dA}{dt} = r_1\,S\,A + r_2\,S\,I - a_1\,A - c_1\,A \\ \frac{dI}{dt} = c_1\,A - a_2\,I - c_2\,I, \\ \frac{dR}{dt} = a_1\,A + a_2\,I, \\ \frac{dD}{dt} = c_2\,I. \end{cases} \tag{1}$$

In this model, we work with five compartments: Susceptible (S), Asymptomatic (A), Symptomatic (I), Recovered (R) and Dead (D). The parameters used are described in the Table (1):

Table 1: Parameters used in the model (1)

Parameter	Meaning	Unit
r_1	Transmission rate of asymptomatic individuals	days^{-1}
r_2	Transmission rate of symptomatic individuals	days^{-1}
a_1	Asymptomatic recovery rate	days^{-1}
a_2	Symptomatic recovery rate	days^{-1}
c_1	Rate at which the asymptomatic individuals become symptomatic	days^{-1}
c_2	Rate of death associated to COVID-19 symptoms	days^{-1}

Therefore, the susceptible individuals get infected by asymptomatic and symptomatic persons at rates r_1 and r_2, respectively. Initially all infected individuals belong to compartment A, which can recover, and no longer infect people at a rate a_1, or become symptomatic, and go to compartment I at a rate c_1. Symptomatic individuals can recover at a rate a_2, entering the compartment R or die, because of COVID-19, at rate c_2, entering compartment D.

Within the concepts of mathematical modeling, the initial conditions are essential parameters to be determined. In this way the initial condition of susceptible $S(0) = S_0$ can be less than the total population (N), since, depending on the adherence to isolation measures, we can have $N > S_0$.

It is possible to say that $\alpha_1 = a_1 + c_1$ is the inverse of τ_1, which is the average period that the individual spends in the A compartment. Also, $\alpha_2 = a_2 + c_2$ as the inverse of τ_2, which is the average time the individual remains in I. Since we are assuming that asymptomatic individuals will be detected when they have symptoms, the fatality rate is given by the total deaths divided by the total infected $m = \frac{c_1}{\alpha_1}\frac{c_2}{\alpha_2}$ (CHICCHI et al., 2020).

Considering $m = 0.029$ (BRASIL, 2021) and the mean incubation and death periods are, respectively, $\tau_1 = 5$ days and $\tau_2 = 11$ days. We can say that:

$$
\begin{aligned}
c_1 &= \alpha_1 - a_1,\\
c_2 &= m\frac{\alpha_1\,\alpha_2}{c_1} = m\frac{\alpha_1\,\alpha_2}{\alpha_1 - a_1},\\
a_2 &= \alpha_2 - c_2 = \alpha_2 - m\frac{\alpha_1\,\alpha_2}{\alpha_1 - a_1}.
\end{aligned}
$$

Thus, there are two parameters to be estimated a_1, r_1, r_2 and two initial conditions S_0 and $A(0) = A_0$, transforming the ODE (1) into:

$$
\left\{
\begin{array}{lcc}
\frac{dS}{dt} &=& -r_1\,S\,A - r_2\,S\,I,\\
\frac{dA}{dt} &=& r_1\,S\,A + r_2\,S\,I - \alpha_1\,A,\\
\frac{dI}{dt} &=& (\alpha_1 - a_1)\,A - \alpha_2\,I,\\
\frac{dR}{dt} &=& a_1\,A + \left(\alpha_2 - m\frac{\alpha_1\,\alpha_2}{\alpha_1 - a_1}\right) I,\\
\frac{dD}{dt} &=& m\frac{\alpha_1\,\alpha_2}{\alpha_1 - a_1}\,I.
\end{array}
\right. \tag{2}
$$

3 Fractional mathematical modeling of COVID-19

Fractional Calculus is defined as the field of mathematical analysis that studies applications of arbitrary order integrals and derivatives. Currently, the interest in fractional calculus is well being stimulated by applications in numerical analysis and in different areas (CAMARGO; OLIVEIRA, 2015).

Since the purpose of mathematical modeling is to describe reality through equations, so that the closer to reality this modeling is, we can somehow predict certain behaviors. In this sense, the difficulties of building a model consistent with reality are many. As much as we add more terms and make the mathematical model more refined, we may still be far from a faithful representation of the situation in practice.

In this way, fractional modeling in many cases demonstrates a more accurate description of the phenomenon analyzed than whole-order modeling. Atangana (ATANGANA, 2016) presents a wide-range temporal or spatial dependence phenomena that can be better described with fractional calculation. In contrast it is rarely possible to analyze these phenomena in such a refined way in the integer order models. It is also possible to embed in the order of the derivative some of the effects of neglected terms in the usual modeling (ARAFA; HANAFY; GOUDA, 2016; CAMARGO; CHARNET; OLIVEIRA, 2009; CAMARGO; OLIVEIRA; VAZ, 2012; CAMARGO; OLIVEIRA, 2015; DEBNATH, 2003; MAINARDI, 2010; ORTIGUEIRA; MACHADO, 2015; DAVID; QUINTINO; SOLIANI, 2013).

There are many definitions and generalizations of fractional operators, but in this work we will use the Riemann-Liouville integral and the Caputo derivative.

3.1 Generalized Adams-Bashforth-Moulton method for fractional models

Fractional modeling plays an outstanding role in the field of applied mathematics to describe certain phenomena. To use fractional modeling, it is usual to change the order of the classic model by a non-integer order smaller than the original. So, it is necessary to look for solving techniques for fractional differential equations (FDE), in case the equations are linear, the methodology of integral transforms is sufficient for the solution. However, most modeling problems are non-linear and cannot be solved by this methodology, for this class of models the solutions are obtained through numerical methods (KURODA et al., 2019).

The low diversity of numerical methods for fractional solutions lays on the fact that non-integer order derivatives are non-local operators, *i.e,* $D^{\alpha} f(t)$ depends on all values of $f(t))$ in every analyzed interval $[t_0, t_f]$, *i.e,* the entire history of the function, in contrast to the classical derivative is a local operator, which only analyzes in an arbitrary neighborhood of the point (DIETHELM; FREED, 1998).

In the literature there are some numerical methods aimed at fractional modeling. In this work we will use the fractional generalization of the classical method of Adams-Bashforth-Moulton (GORENFLO, 1997). This numerical method in its fractional version is developed with the derivative in the Caputo sense, considering the non-integer order of the fractional derivative, $m - 1 < \alpha \leq m$, where m is the smallest integer greater than α. Let the non-integer order initial value problem be:

$$D^{\alpha}_{t_0}(y)(t) = f(t,\, y(t)), \quad t_0 \leq t \leq t_f. \tag{3}$$

It is possible to transform the equation (3) into a Volterra's integral with the weakly singular nucleus (LI; TAO, 2009; DIETHELM; FREED, 1998), using the arbitrary order of the derivative $0 < \alpha \leq 1$:

$$y(t) = y_0 + \frac{1}{\Gamma(\alpha)} \int_{t_0}^{t} (t - \tau)^{\alpha - 1} f(\tau,\, y(\tau))\, d\tau. \tag{4}$$

So, the key to the derivation of the Adams-Bashforth-Moulton method to its fractional version is to transform the original fractional differential equation (FDE) by a Volterra equation and implement the integration method for the Volterra integral.

3.2 Fractional generalization

In order to propose the fractional generalization for the classical SAIRD model of system (1) equation, we must be careful with the unbalance of the dimensions of the units of the differential equation. When we introduce the derivative of non-integer order as the operator:

$$\frac{d^{\beta}}{dt^{\beta}},$$

with $0 < \beta \leq 1$, which is the non-integer order. When $\beta = 1$ we obtain the classical derivative as a particular case of the fractional operator. In the case of the integer order derivative, the operator has dimension of the inverse of days, $\frac{1}{\text{days}}$, since in our particular case of COVID-19 dynamic modeling we analyze the data in periods of days, but in the fractional operator we have that

$$\left[\frac{d^{\beta}}{dt^{\beta}}\right] = \frac{1}{\text{days}^{\beta}}, \quad 0 < \beta \leq 1.$$

It is noteworthy that in this work we use [ ] as the notation for the unit of measure.

To maintain consistency with dimensionality, we can introduce a new parameter τ, where $[\tau]$ = days, so that:

$$\left[\frac{1}{\tau^{1-\beta}}\frac{d^\beta}{dt^\beta}\right] = \frac{1}{\text{days}} = \left(\frac{1}{\text{days}}\right)^{1-\beta} \times \left(\frac{1}{\text{days}}\right)^{\beta} = \frac{1}{\text{days}}. \tag{5}$$

In the equation (5) if $\beta = 1$, the classical model is recovered. Therefore, we can perform the fractional generalization of the (1) model, dimensionally adjusting the fractional operator adding the parameter τ:

$$\frac{d}{dt} \rightarrow \frac{1}{\tau^{1-\beta}}\frac{d^\beta}{d\,t^\beta}, \quad 0 < \beta \leq 1, \tag{6}$$

Therefore, the fractional version of the ODE system (2) is given by

$$\begin{cases} \frac{d^\beta S}{d\,t^\beta} &= \tau^{1-\beta}(-r_1\,S\,A - r_2\,S\,I) \\ \frac{d^\beta A}{d\,t^\beta} &= \tau^{1-\beta}(r_1\,S\,A + r_2\,S\,I - -\alpha_1\,A), \\ \frac{d^\beta I}{d\,t^\beta} &= \tau^{1-\beta}((\alpha_1 - a_1)\,A - \alpha_2\,I), \\ \frac{d^\beta R}{d\,t^\beta} &= \tau^{1-\beta}(a_1\,A + \left(\alpha_2 - m\frac{\alpha_1\,\alpha_2}{\alpha_1 - a_1}\right)I), \\ \frac{d^\beta D}{d\,t^\beta} &= \tau^{1-\beta}\left(m\frac{\alpha_1\,\alpha_2}{\alpha_1 - a_1}\,I\right). \end{cases} \tag{7}$$

In the next section, we propose different assumptions and strategies to fit both the classical SAIRD model and its fractional version to reported data of COVID-19 cases and deaths. Then, we compared the fitting result and the accuracy of the models.

4 Computational strategies

In the classic model (2), it is necessary to estimate three model parameters: a_1, the recovery rate for asymptomatic individuals, r_1, the infection rate for asymptomatic individuals, and r_2, the infection rate for symptomatic individuals. In addition of these parameters, we can consider the two initial conditions S_0 and A_0 as parameters to be estimated.

In the classical computational strategy A, we considered that symptomatic individuals isolate themselves and, therefore, they do not transmit the disease, $r_2 = 0$. As result, the vector of optimal parameters is $p^* = [S_0,\ E_0,\ a_1,\ r_1]$.In the classical computational strategy B, we will use the $r_2 \neq 0$, so the vector of optimal parameters in this strategy is given by $p^* = [S_0, E_0, a_1, r_1, r_2]$.

When we consider the fractional model (7), besides the parameters S_0, A_0, a_1, r_1 and r_2, it is necessary to estimate the non-integer order of the derivative, β. Thus, for this case, we propose four computational strategies: A_1 and A_2, what vary β in fixed sizes or consider it as a parameter to be estimated, respectively. In both strategies we assume that $r_2 = 0$.

In strategies B_1 and B_2, we vary β in fixed sizes or consider it as a parameter to be estimated, respectively. However, now, in both strategies we consider $r_2 \leq 0$, as parameter to be estimated. And all estimations are made by the Levenberg-Marquardt algorithm using the *lqnonlin* function in MatLab minimizing the mean squared error (MSE), given by:

$$MSE = \sum_{i=1}^{n}\frac{1}{n}(C(i)_{\text{data}} - C(i)_{\text{estimated}})^2 + (D(i)_{\text{data}} - D(i)_{\text{estimated}})^2, \tag{8}$$

considering $C(i)_{\text{data}}$ and $D(i)_{\text{data}}$ as the data of cumulative COVID-19 cases and deaths. $C(i)_{\text{estimated}}$ and $D(i)_{\text{estimated}}$ as the estimated curve of cumulative cases and deaths.

Table 2 summarizes the computational strategies that we used, what is assumed in each one of them and which parameters are estimated.

Table 2: Computational Strategies used in this work

Strategy	Model	Assumption	Estimated parameters (p^*)
A	Classic	$r_2 = 0$	$[S_0, A_0, a_1, r_1]$
B	Classic	$r_2 \neq 0$	$[S_0, A_0, a_1, r_1]$
A_1	Fractional	$r_2 = 0$ and fixed β	$[S_0, A_0, a_1, r_1, \tau]$
A_2	Fractional	$r_2 = 0$ and estimated β	$[S_0, A_0, a_1, r_1, \tau, \beta]$
B_1	Fractional	$r_2 \neq 0$ and fixed β	$[S_0, A_0, a_1, r_1, r_2, \tau]$
A_2	Fractional	$r_2 \neq 0$ and estimated β	$[S_0, A_0, a_1, r_1, r_2, \tau, \beta]$

5 Results

The pandemic scenario in Brazil was analyzed in each computational strategy considering data for the months of April and May, 2020 (COTA, 2020). In those months, we considered the following initial conditions: $I_0 = 6609$, $R_0 = 78$, $D_0 = 244$ and $C_0 = 6931$.

5.1 Classical computational strategy A

In computational strategy A, the vector of optimal parameters is $p^* = [S_0, E_0, a_1, r_1]$, considering the rate of infection by symptomatic individuals, $r_2 = 0$.

Table 3 shows the parameter ranges that were used during the estimation. Also, the vector of initial values for parameters is given by

$$p_0 = [190 \times 10^6, 15 \times 10^3, 0.15, 11 \times 10^{-8}].$$

As can be seen in Figure 2, we were able to achieve a reasonable fitting using this strategy.

Table 3: Range of parameters and initial conditions used for the simulation from April to May 2020.

Parameter	Range
S_0	$[170 \times 10^6,\ 209 \times 10^6]$
A_0	$[1 \times 10^3,\ 6 \times 10^5]$
a_1	$[0.14,\ 0.20]$
r_1	$[1 \times 10^{-9},\ 12 \times 10^{-8}]$

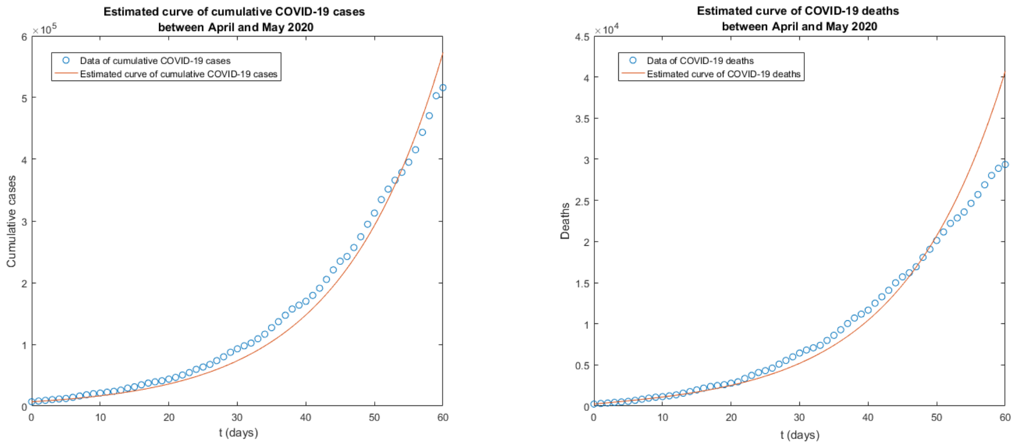

Figure 2: Comparison between real data on cases and deaths because of COVID-19 and the estimation made by the authors in the classical SAIRD model, in the strategy A.

In the classical computational strategy A we obtained a mean squared error of 4.29×10^8.

5.2 Classical computational strategy B

In the computational strategy B, we used $r_2 \neq 0$, considering the rate of infection by symptomatic individuals as a parameter to be estimated. Therefore, the vector of optimal parameters in this strategy is $p^* = [S_0, E_0, a_1, r_1, r_2]$, and their estimation was performed using the ranges presented in Table 3 and the range $[0,\ 12 \times 10^{-8}]$ days^{-1} for r_2. Moreover, the initial value of the parameters vector that was used by the optimization method was $p_0 = [190 \times 10^6, 15 \times 10^3, 0.15, 11 \times 10^{-8},\ 1 \times 10^{-14}]$.

In this case, shown in Figure 3, the MSE was 4.32×10^8, resulting in a worse fitting than in the previous strategy, with 6.99% difference.

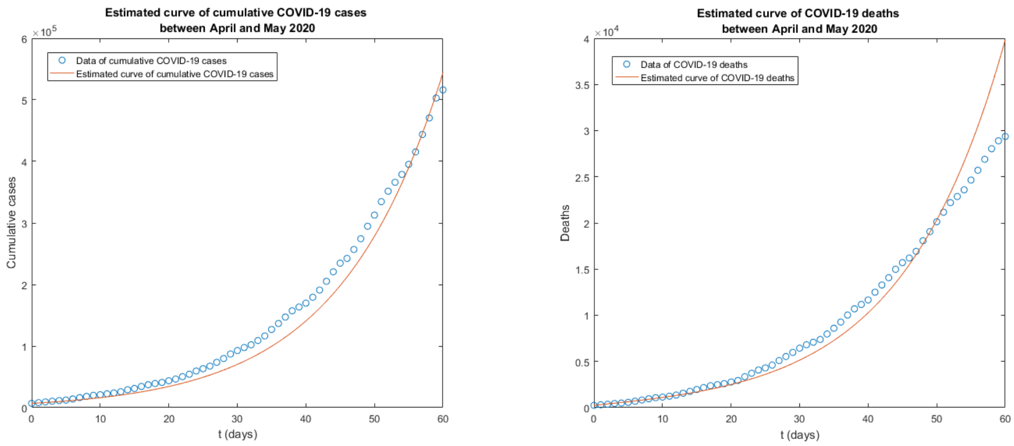

Figure 3: Comparison between real data on cases and deaths because of COVID-19 and the estimation made by the authors in the classical SAIRD model, in the B strategy.

5.3 Fractional computational strategy A_1

In the fractional strategy A_1 varying the value of β from 1 to 0.984, because for values below this threshold, according to our estimations, the mean squared error value started increasing regardless the fitting process. The result of the optimization algorithm can be seen in Table 5, which contains the values of β, the optimal parameter vector, p^*, and the obtained MSE for all the scenarios.

For the estimation in the strategy A_1, where we vary the value of β, we use the following lower and upper limits described in the table 5.3:

Table 4: Range of parameters and initial conditions used for the simulations from April to May 2020 in the computational strategy A_1.

Parameter	Range
S_0	$[170 \times 10^6,\ 209 \times 10^6]$
A_0	$[1 \times 10^3,\ 6 \times 10^5]$
a_1	$[0.14,\ 0.20]$
r_1	$[1 \times 10^{-9},\ 12 \times 10^{-8}]$
τ	$[0.1, 3]$

For the vector of the initial values of the parameters, it was used

$$p_0 = [190 \times 10^6,\ 15 \times 10^3,\ 0.15,\ 11 \times 10^{-8},\ 2.4].$$

Table 5: Values of β with their respective optimal parameter vectors and the mean squared error obtained in the simulations.

β	p^*	MSE
1	$[1.87 \times 10^8,\ 1.40 \times 10^4,\ 0.154,\ 1.44 \times 10^-9,\ 2.4]$	4.29×10^8
0.998	$[1.85 \times 10^8,\ 1.46 \times 10^4,\ 0.153,\ 1.44 \times 10^-9,\ 1.95]$	3.89×10^8
0.996	$[1.83 \times 10^8,\ 1.77 \times 10^4,\ 0.155,\ 1.43 \times 10^-9,\ 1.69]$	3.02×10^8
0.994	$[1.83 \times 10^8,\ 1.77 \times 10^4,\ 0.154,\ 1.43 \times 10^-9,\ 2.06]$	2.95×10^8
0.992	$[1.83 \times 10^8,\ 1.79 \times 10^4,\ 0.154,\ 1.43 \times 10^-9,\ 2.05]$	2.71×10^8
0.990	$[1.83 \times 10^8,\ 1.81 \times 10^4,\ 0.154,\ 1.43 \times 10^-9,\ 2.05]$	2.5×10^8
0.988	$[1.86 \times 10^8,\ 1.55 \times 10^4,\ 0.153,\ 1.43 \times 10^-9,\ 2.13]$	3.41×10^8
0.986	$[1.83 \times 10^8,\ 1.59 \times 10^4,\ 0.153,\ 1.43 \times 10^-9,\ 2.1]$	3.25×10^8
0.984	$[1.87 \times 10^8,\ 1.49 \times 10^4,\ 0.154,\ 1.43 \times 10^-9,\ 2.17]$	3.19×10^8

We can observe from Table 5, that the simulation where $\beta = 0.990$ was the one that fitted better to the real data, obtaining a mean square error of 2.5×10^8, lower than the other values.Thus, Figure 4 shows the estimated curves of cumulative cases and deaths by COVID-19 using the strategy A_1, with $\beta = 0.99$.

5.4 Fractional computational strategy A_2

In the strategy A_2, we wanted to estimate of the non-integer order of the derivative, β. In this case, as its initial value, we used the best estimated value obtained in the strategy A_1, which was $\beta = 0.99$. Therefore, the vector of initial values used in the optimization method is

$$p_0 = [190 \times 10^6,\ 15 \times 10^3,\ 0.15,\ 11 \times 10^{-8},\ 2.4,\ 0.99].$$

In this strategy A_2, the MSE was 2.32×10^8. We can say that there were no very noticeable differences in the final result, nor in the mean squared error in using any of the strategies A_1 or A_2,

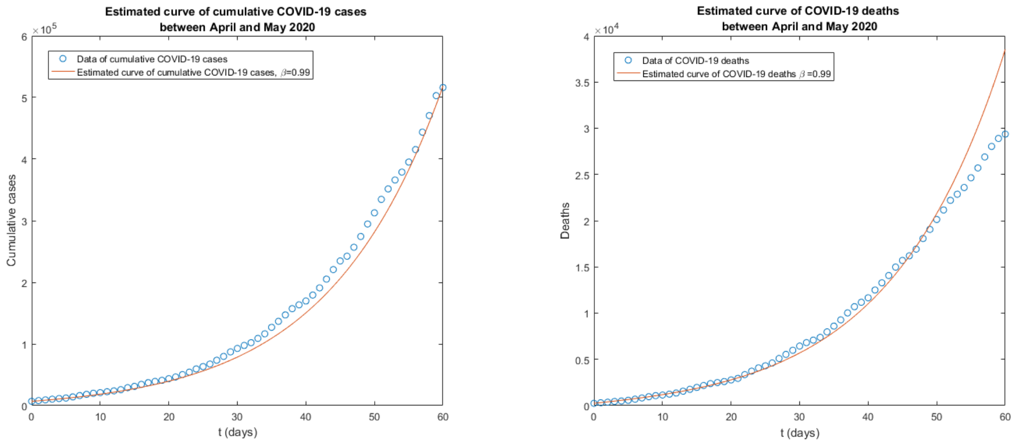

Figure 4: Comparison between real data on cases and deaths because of COVID-19 and the estimation made by the authors in the fractional SAIRD model, in the A_1 strategy, using $\beta = 0.99$.

i.e, fixing the non-integer order of the derivative or estimating the order of the derivative. Figure 5 displays the estimated curves of cumulative cases and deaths, respectively using the computational strategy A_2. The range of parameters was the same as the table 5 including the range of β, $\beta \in [0.98,\ 0.9999]$

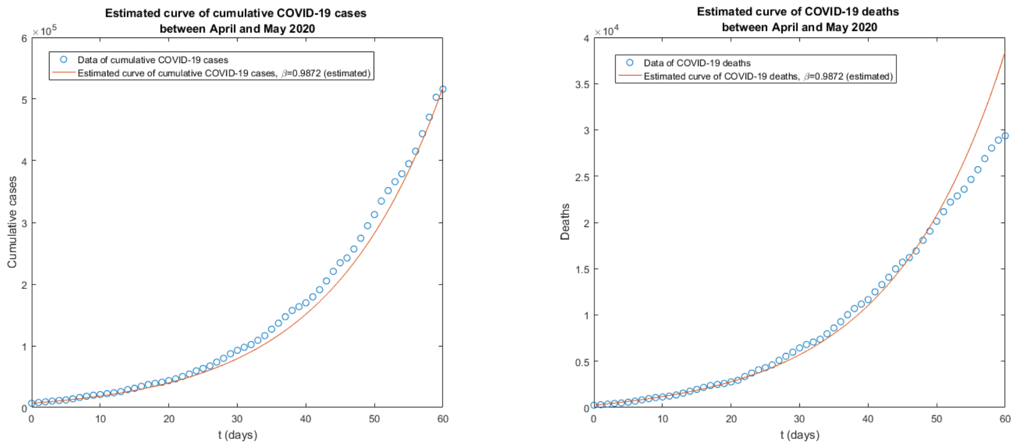

Figure 5: Comparison between real data on cases and deaths because of COVID-19 and the estimation made by the authors in the fractional SAIRD model, in the A_2 strategy, using $\beta = 0.9872$.

5.5 Fractional computational strategy B_1

In the B_1 fractional estimation strategy, we consider the symptomatic infection rate as a parameter to be estimated, *i.e.,* $r_2 \neq 0$, in addition to the non-integer order of the derivative β that is varied with fixed step, $h = 0.002$, from 1 to 0.984, because for values of β below 0.984 the mean squared error value increased much more than in the classic model.

Table 6 shows the values of β, the estimated parameter vector, p^*, and the obtained mean squared error value, MSE, for this strategy B_1.

We can see from Table 6 that the simulation in the strategy B_1 where $\beta = 0.994$ presented a better fitting to the reported data, obtaining a mean square error of 6.13×10^7. We can also observe the

Table 6: Values of β with their respective optimal parameter vectors and the mean square error obtained in the simulations.

β	p^*	MSE
1	$[1.87\times 10^8,\ 1.38\times 10^4,\ 0.155,\ 1.44\times 10^{-}9,\ 2.7\times 10^{-14},\ 2.4]$	4.32×10^8
0.998	$[1.86\times 10^8,\ 1.6\times 10^4,\ 0.153,\ 1.42\times 10^{-}9,\ 2.22\times 10^{-14},\ 2.14]$	2.91×10^8
0.996	$[1.84\times 10^8,\ 1.73\times 10^4,\ 0.155,\ 1.43\times 10^{-}9,\ 2.59\times 10^{-14},\ 1.57]$	3.20×10^8
0.994	$[1.82\times 10^8,\ 2\times 10^4,\ 0.151,\ 1.42\times 10^{-}9,\ 2.84\times 10^{-14},\ 1.94]$	6.13×10^7
0.992	$[1.87\times 10^8,\ 1.43\times 10^4,\ 0.153,\ 1.43\times 10^{-}9,\ 2.43\times 10^{-14},\ 2.13]$	5.04×10^8
0.99	$[1.83\times 10^8,\ 1.81\times 10^4,\ 0.154,\ 1.43\times 10^{-}9,\ 2.34\times 10^{-14},\ 2.05]$	2.50×10^8
0.988	$[1.86\times 10^8,\ 1.55\times 10^4,\ 0.153,\ 1.43\times 10^{-}9,\ 2.86\times 10^{-14},\ 2.13]$	3.41×10^8
0.986	$[1.88\times 10^8,\ 1.46\times 10^4,\ 0.152,\ 1.43\times 10^{-}9,\ 2.84\times 10^{-14},\ 2.23]$	3.02×10^8
0.984	$[1.86\times 10^8,\ 1.61\times 10^4,\ 0.153,\ 1.43\times 10^{-}9,\ 2.38\times 10^{-14},\ 2.14]$	3.08×10^8

accuracy of this strategy in Figure 6, where we have the cumulative cases and deaths by COVID-19 using the strategy B_1, with $\beta = 0.994$.

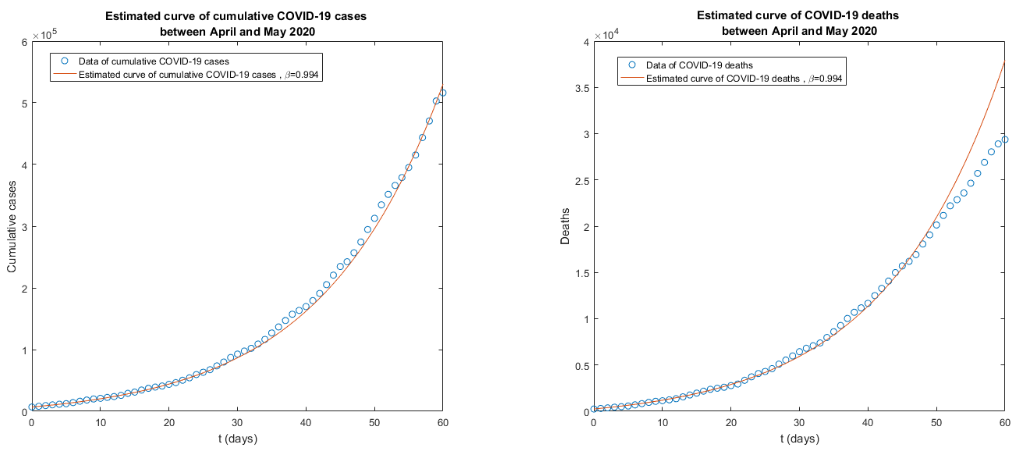

Figure 6: Comparison between real data on cases and deaths because of COVID-19 and the estimation made by the authors in the fractional SAIRD model, in the B_1 strategy, using $\beta = 0.994$.

5.6 Fractional computational strategy B_2

The strategy B_2 was, analogous to A_2, performed using the derivative order as a parameter to be estimated. As initial value for β, we used the best result of strategy B_1, as before. Therefore, the vector of initial values of the parameters is

$$p_0 = [190\times 10^6, 15\times 10^3, 0.15, 11\times 10^{-8},\ 1\times 10^{-14},\ 2.4,\ 0.994].$$

With this computational strategy we obtained a MSE of 2.797×10^8, which is close to those obtained in the Table 6, but higher than the smallest error obtained by the strategy B_1.It can be concluded that within strategy B, the strategy B_1 obtained a smaller error regarding the available data on cumulative cases and deaths than the B_2 strategy, where the order of the non-integer derivative was estimated. We can see in Figure 7 the cumulative cases and deaths by COVID-19 using the strategy B_2

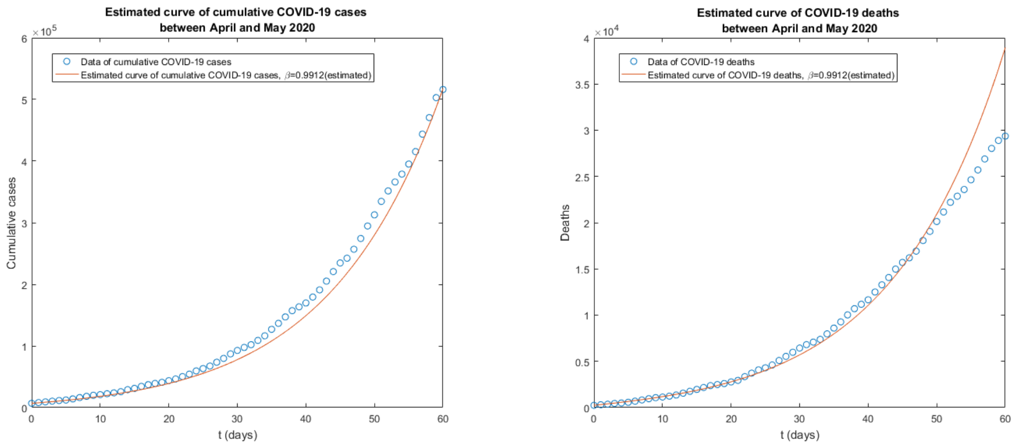

Figure 7: Comparison between real data on cases and deaths because of COVID-19 and the estimation made by the authors in the fractional SAIRD model, in the B_2 strategy, using $\beta = 0.9912$.

6 Conclusion

In (CHICCHI et al., 2020), the model (2) was used both in the classic model and in the fractional generalization, the present work tried to use this same classic model, but for the fractional generalization we performed the dimensional adjustment through the parameter τ to maintain consistency with dimensionality in the fractional differential equation. In this way, we estimate the redimensionalization parameter, τ, together with the other model parameters and the non-integer order of the derivative in the case of the strategies A_2 and B_2.

In this same work (CHICCHI et al., 2020), the authors performed the comparison analysis between the classic and fractional SAIRD model through the RMSE (root mean squared error). In our work we use a comparison measure similar to the RMSE, which also evaluates the difference between an estimator and the true value of the estimated quantity, which is the MSE (mean squared error).

From the numerical simulations, an analysis was performed by comparing the order of the derivative and the mean square error produced between the estimated curve and available data on cumulative cases and deaths from COVID-19. Through all simulations and comparisons, it was possible to observe that in the fractional model the estimated curves came closer to the reported data (COTA, 2020). Furthermore, although we subdivided the computational strategies between fixing and estimating the order of the derivative, there was no significant change in the mean square errors obtained among the fractional strategies.

The importance of the present work is to carry out a numerical analysis through comparisons between the classical model and its fractional generalizations with the main objective of trying to embed the effects of simplifications in the models in the non-integer order of the derivative.

References

ARAFA, A. A. M.; HANAFY, I. M.; GOUDA, M. I. Stability analysis of fractional order hiv infection of $^+$t cells with numerical solutions. **Journal of Fractional Calculus and Applications**, Alexandria, v. 7, n. 1, p. 36–45, 2016.

ATANGANA, A. Application of fractional calculus to epidemiology. *In*: CATTANI, C.; SRIVASTAVA, H. M.; YANG, X-J. **Fractional Dynamics**. Berlin: De Gruyter Open Poland, 2016. p. 174–190.

BRASIL. **Painel Coronavírus**. Brasília-DF: Ministério da Saúde, 2021. Disponível em: <https://covid.saude.gov.br/>. Acesso em: 05 dez. 2021.

CAMARGO, R. F.; CHARNET, R.; OLIVEIRA, E. C. On some fractional green's functions. **Journal of Mathematical Physics**, New York, v. 50, n. 4, p. 043514, 2009.

CAMARGO, R. F.; OLIVEIRA, E. C. **Cálculo fracionário**. São Paulo: Editora Livraria da Fısica, 2015.

CAMARGO, R. F.; OLIVEIRA, E. C.; VAZ, J. On the generalized mittag-leffler function and its application in a fractional telegraph equation. **Mathematical Physics, Analysis and Geometry**, New York, v. 15, n. 1, p. 1–16, 2012.

CHAKRABORTY, I.; MAITY, P. Covid-19 outbreak: migration, effects on society, global environment and prevention. **Science of the Total Environment**, Amsterdam, v. 728, 2020.

CHICCHI, L. et al. First results with a seird model. Quantifying the population of asymptomatic individuals in italy. **Preprint on ResearchGate**, 2020. Disponível em: <http://www.researchgate.net/project/Analysis-and-forecast-of-COVID-19-spreading>. Acesso em: 30 set. 2021.

COTA, W. Monitoring the number of COVID-19 cases and deaths in brazil at municipal and federative units level. **SciELOPreprints:362**, FapUNIFESP (SciELO), may 2020. Disponível em: <https://doi.org/10.1590/scielopreprints.362>. Acesso em: 30 set. 2021.

DAVID, S. A.; QUINTINO, D. D.; SOLIANI, J. Fractional-order in a macroeconomic dynamic model. **AIP Conference Proceedings**, New York, v. 1558, n. 1, p. 2142–2146, 2013.

DEBNATH, L. Recent applications of fractional calculus to science and engineering. **International Journal of Mathematics and Mathematical Sciences**, Hindawi, v. 2003, n. 54, p. 3413–3442, 2003.

DIETHELM, K.; FREED, A. D. The fracpece subroutine for the numerical solution of differential equations of fractional order. **Forschung und wissenschaftliches Rechnen**, Germany, v. 1999, p. 57–71, 1998.

GORENFLO, R. Fractional calculus: some numerical methods. **Courses and lectures-international centre for mechanical sciences**, Berlim, p. 277–290, 1997.

KISS, I. Z.; MILLER, J. C.; SIMON, P. L. **Mathematics of Epidemics on Networks**: from exact to approximate models. Switzerland: Springer International Publishing, 2017.

KURODA, L. K. B. et al. Análise do método multi-passos com transformada diferencial generalizada na modelagem fracionária. **TEMA**, São Carlos, v. 20, n. 1, p. 133–147, 2019.

LI, C.; TAO, C. On the fractional adams method. **Computers & Mathematics with Applications**, Amsterdam, v. 58, n. 8, p. 1573–1588, 2009.

MAINARDI, F. **Fractional Calculus and Waves in Linear Viscoelasticity**: an introduction to mathematical models. [S.l.]: World Scientific, 2010.

ORTIGUEIRA, M. D.; MACHADO, J. T. What is a fractional derivative? **Journal of computational Physics**, Amsterdam, v. 293, p. 4–13, 2015.

SANTOS, W. G. Natural history of covid-19 and current knowledge on treatment therapeutic options. **Biomedicine** & **Pharmacotherapy**, Paris, v. 129, n. 110493, p. 1–18, 2020.

WU, Y. C.; CHAN, Y. J. The outbreak of covid-19: an overview. **Journal of Chinese Medical Association**, Taiwan, v. 83, 2020.